Universiteit Antwerpen

This item is the archived peer-reviewed author-version of:

An innovative air purification method and neural network algorithm applied to urban streets

Reference:
Boumahdi Meryenne, El Amrani Chaker, Denys Siegfried.- An innovative air purification method and neural netw ork algorithm applied to urban streets
International journal of embedded and real-time communication systems - ISSN 1947-3184 - 10:4(2019), p. 1-19
Full text (Publisher's DOI): https://doi.org/10.4018/IJERTCS.2019100101
To cite this reference: https://hdl.handle.net/10067/1625950151162165141

uantwerpen.be
Institutional repository IRUA

An Innovative Air Purification Method and Neural Network Algorithm Applied to Urban Streets

Meryeme Boumahdi, University Abdelmalek Essaadi, Tétouan, Morocco
Chaker El Amrani, University Abdelmalek Essaadi, Tétouan, Morocco
Siegfried Denys, University of Antwerp, Research Group Sustainable Energy, Air and Water Technology, Antwerp, Belgium

ABSTRACT

In the present work, multiphysics modeling was used to investigate the feasibility of a photocatalysisbased outdoor air purifying solution that could be used in high polluted streets, especially street canyons. The article focuses on the use of a semi-active photocatalysis in the surfaces of the street as a solution to remove anthropogenic pollutants from the air. The solution is based on lamellae arranged horizontally on the wall of the street, coated with a photocatalyst (TiO2), lightened with UV light, with a dimension of 8 cm × 48 cm × 1 m. Fans were used in the system to create airflow. A high purification percentage was obtained. An artificial neural network (ANN) was used to predict the optimal purification method based on previous simulations, to design purification strategies considering the energy cost. The ANN was used to forecast the amount of purified with a feed-forward neural network and a backpropagation algorithm to train the model.

Keywords: CFD, Comsol, Matlab, Modeling, MSG, Neural Network, Photocatalysis

INTRODUCTION

Most cities in the world suffer from air pollution, due several many factors such as burning fuel, industry and release of chemicals (Kurt 2016, Li 2012, Li 2017). Many studies have focused on reducing emissions of pollutants, with significant progress being made. So far, large part of the population in urban areas breathe air, that does not meet European standards nor the World Health Organisation Air Quality Guidelines (Kelly 2015). Currently, there is no ready-to-use technology available for a sustainable removal of particulate matter (PM), Nitric Oxides (NOx), nor volatile organic compounds (VOCs), in an urban environment. The photocatalytic oxidation (PCO) has been the focus of increasing attention in recent years, to abate pollutants, with possible applications in several areas, including environmental and energy related areas. The Titanium dioxide (TiO2) used as photocatalysts, is almost the only material suitable in industry at present and also probably in the future (Paz 2010, Mamaghani 2017). The choice of TiO2 is based on the highest stability, low cost, and transparency to visible light and a high efficient photoactivity (Ribeiro 2013). PCO is particularly useful for volatile organic compounds (VOC's), but according to the literature, the NOx can also be degraded to a lesser extent (to nitrogen). Furthermore, TiO2 is also known to degrade the organic fraction of particulate matter (black carbon, soot). The latter is proven by many papers evidencing the self-cleaning properties of TiO2 (Bianchi 2015).
In the last decades, thanks to advances made in computational resources, numerical simulation approaches have become increasingly popular. Nowadays, simulations with Computational Fluid Dynamics (CFD) is frequently used to assess urban microclimate.
Several research in artificial neural networks (ANNs) show that ANNs have powerful pattern classification and pattern recognition capabilities and they are used in many fields. They have become well established as viable, multipurpose, robust computational methodologies with solid theoretic support and with strong potential to be effective in any discipline (Dayhoff 2001). Inspired by the biological system, especially the sophisticated functionality of human brains where hundreds of billions of interconnected neurons process information in parallel (Wang 2003). ANNs algorithms are able to learn and generalize from examples and experiences as they have the ability to capture functional relationships among the data, even if the relationships are hard to describe or they are unknown. The advantage of

using ANNs is that they minimize the error compared to other forecasting methods, and they provide results that are approximately close to analytical values.
Recent studies focusing on outdoor pollution show that the most important problem in the urban environment is the lack of urban ventilation. In this context, the proposed solution in this work focuses on the improvement of the contact with photocatalytic surfaces, taking advantage from the self-cleaning properties of TiO2. In this paper, a new solution for outdoor air purification based on semi-active photocatalysis is described.We present an innovative solution for outdoor air purification, using photocatalysis technology. This technology is based on coated lamellas with TiO2, lighted with UV light and placed horizontally on the buildings, in streets, using forced convection with a fan to force polluted air over the system. Natural convection was tested to in order to reduce the energy cost. It replaces the airflow generated by the fans, with an airflow produced by the density difference of the air between the lamellas. Considering the complexity of the interactions involved, a modelling approach is the designated approach to follow. In the present work, air flow, adsorption / desorption and photocatalytic reactions were studied using commercial computational fluid dynamics (CFD) software.

The first section of the paper provides a literature review and related work on photocatalysis properties and its use on air purification. The Multiphysics modeling section explains in details the use of CFD and the geometry that was used for the model, the airflow modeling, and adsorption and desorption equations used to model the system. The next section presents the use of the simulation, not only to test the efficiency of the method but also to train other machine learning algorithms to predict the purification behavior for other streets. It explains the reason why IA was used in this study and some mathematical formulas that were used in the feed-forward neural network. Finally, results are, presented obtained from the simulations using CFD, and the results obtained from the neural network model.

Table 1. Nomenclature

D mass diffusion coefficient of acetaldehyde in air ($m^2\ s^{-1}$)	K Langmuir equilibrium constant ($m^3\ mol^{-1}$)
u stationary velocity field vector ($m\ s^{-1}$)	K_{ads} adsorption rate constant ($m\ s^{-1}$)
n normal vector pointing outward on the boundaries of the geometry	K_{des} desorption rate constant ($mol\ m^{-2}\ s^{-1}$)
θ_{Acal} fractional surface coverage	k_{pco} photocatalytic reaction rate constant (s^{-1})
Γ_s maximum surface coverage ($mol\ m^2$)	R_{pco} photocatalytic reaction rate ($mol\ m^{-2}s^{-1}$)
C_{ads} surface concentration of acetaldehyde ($mol\ m^{-2}$)	N_{ads} adsorption flux of acetaldehyde ($mol\ m^{-2}s^{-1}$)
	N_{des} desorption flux of acetaldehyde ($mol\ m^{-2}s^{-1}$)
	C_{VOCs} concentration of ($mol\ m^{-3}$)

RELATED WORK

The PCO principle is based on a semiconductor type of reaction: photons with sufficient energy - in the UV range -, hitting the TiO_2, cause electrons from the valence band to move to the conduction band. So, when photocatalyst titanium dioxide (TiO_2) absorbs Ultraviolet (UV)* radiation from sunlight or illuminated light source (fluorescent lamps), it will produce pairs of electrons and holes. The electron of the valence band of titanium dioxide becomes excited when illuminated by light. The excess energy of this excited electron promoted the electron to the conduction band of titanium dioxide, therefore, creating the negative-electron (e-) and positive-hole (h+) pair. Both electrons and holes can then cause oxidation and reduction reactions, causing both water and oxygen molecules to form very reactive radicals such as the hydroxyl radical (HO•) and $•O_2−$ radicals. These oxidation / reduction reactions take place at the surface (in fact, H2O and O2 should be adsorbed on the surface, hence the O_{2ads} notation). In the presence

of air or oxygen, UV-irradiated TiO_2 is capable of destructing many organic contaminants completely (Zhao 2003). The activation of TiO2 by UV light can be written as:

$$TiO_2 + h\nu \rightarrow h+ + e-$$

In this reaction, h+ and e− are powerful oxidizing and reductive agents, respectively. The oxidative and reductive reactions are expressed as:
Oxidative reaction:

$$h+ + H_2O \rightarrow H+ + \bullet OH$$

Reductive reaction:

$$O_{2ads} + e- \rightarrow \bullet O_2-$$

For a complete PCO reaction, the final products of reactions are CO_2 and H_2O.

$$OH^* + \text{pollutant} + O_2 \rightarrow \text{Products } (CO_2; H_2O; \text{etc.})$$

Today, the main application field of PCO lies in end-of-pipe active PCO reactors in which polluted air is forced over a photocatalytic surface. Unfortunately, contradicting results exist concerning the efficiency of passive decontamination surfaces (paving, walls and facades treated with a photocatalyst to clean air) in the real urban atmosphere (so-called passive PCO). Concluded from different field data of the Life+ project PhotoPAQ that a realistic annual average NOx reduction of 2% can be expected in main urban street canyons exceeding the European annual NO_2 threshold limit value of 40 $\mu g.m^{-3}$. The limitations of passive decontamination surfaces in urban environments are not surprising. Firstly, as mass transport is often limited, only a fraction of the photocatalytic degradation potential is used (Paz 2010). Secondly, passive systems are often based on solar light, and thus depend on the sun cycle. Furthermore, common photocatalysts are primarily metal oxides and sulphides and require UV light for their activation. A lot of research is being done to shift the activity of photocatalysts to the visible light spectrum, with varying success.
Compared to conventional air cleaning technologies, such as adsorption and filtration, PCO can target several air pollutants, does not pose a disposal issue and uses a sustainable energy source. Furthermore, the process is operated at ambient conditions, i.e. room temperature, and works best at typical low concentration levels (ppb or ppm) of polluted air. Several air cleaning methods are available on the market. Technologies as condensation ionization and incineration cannot control emissions and improve air quality, thus, these technologies degrade air quality (Ranjit 2016). Filtration technologies are the most widely used methods for air cleaning, they are known by the low cost and high pollutant removal effectiveness. But they are associated with health issues by increasing the pollutant concentration. In this context Heterogeneous photocatalysis with titanium dioxide (TiO_2) as a catalyst is a rapidly developing field in environmental engineering, as it has a great potential to cope with the increasing pollution, besides its self-cleaning properties.

A solution for the air by traffic can be found in the treatment of the pollutants as close as possible from the source (Chen 2009). There are different steps for the air purification through heterogeneous photocatalysis: under the influence of UV-light, the photoactive TiO_2 at the surface of the material is activated. One of the solutions that applied the photocatalysis in outdoor air purification using titanium dioxide was based on photocatalytic concrete paving blocks. Finally, they can be removed from the surface by the rain or cleaning/washing with water. This technology removes around 15% of NO (Boonen 2014, Srivastava 2015).

MULTIPHYSICS MODELING

Geometry

The proposed method in this work is based on lamellae coated with TiO_2 with the dimension of 8cm*48cm*1m. Lightened with UV light. The rotation of the lamellae is 45° to guarantee the air flow in the system. A constant VOCs background concentration was used $10^{-4} mol/m^3$. Three different flow rate

were tested at 0.1 m^3/s, 0.5 m^3/s and 1 m^3/s with a pressure of 100 Pa, to see the difference between the air velocity and the VOCs concentration. A concentration equal to the initial condition was considered in the open boundaries. On the top, open boundaries are considered (air can leave or enter the geometry through open boundaries). The boundary condition there is a specific pressure and should be chosen sufficiently far from the buildings Figure 1.

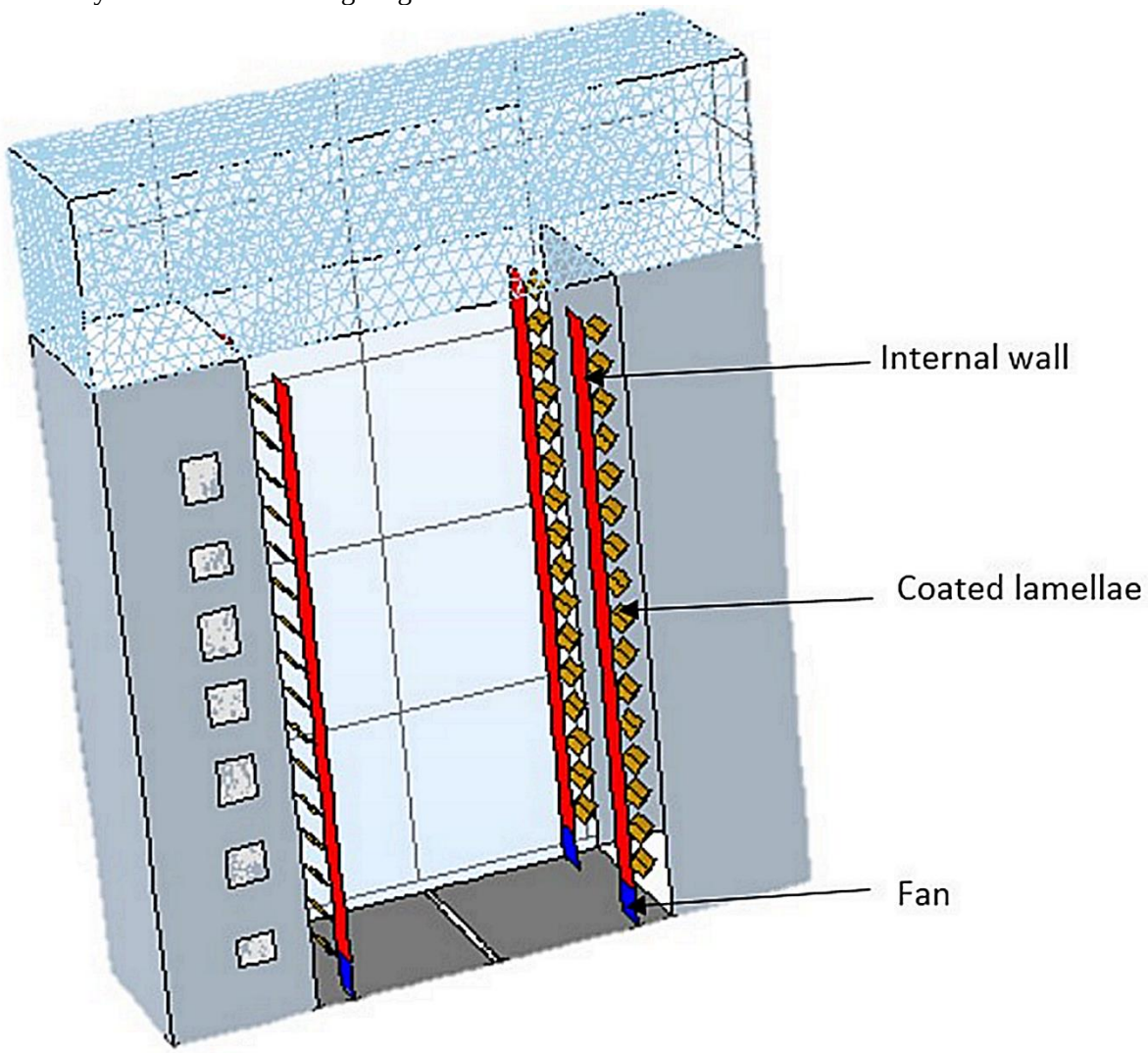

Figure 1. Geometry of the proposed method based on coated lamellae

Air flow modeling

The commercial software package Comsol Multiphysics v.5.3 was used to perform all theoretical simulations. In this work, several models provided by Comsol were used. Computational fluid dynamics model was used to simulate the air flow generated by the fans (Hanna 2006,Buccolieri 2011, Toparlar 2017, Whong 2016, Blocken 2016, García-Sánchez 2018) . Transport of diluted species model was used for the chemical reactions happened in the coated surfaces. LiveLink for Matlab model was used in order to connect Comsol to Matlab and to transfer all the simulation data to Matlab. A 2D model was used instant of a 3D model to reduce computational time and also resources. A test mesh was used in the model; the meshes used were gradually refined until they do not affect the results. The finer mesh was required in certain places to guarantee the efficiency in the model and all the chemical and photocatalysis reactions happened in the surface of the lamellae. A user-defined mesh was used there to guarantee good results and

a total number of 53,680 triangles were needed to guarantee a sufficiently fine mesh for the model (Figure 2).

Local Reynolds numbers were low under the studied conditions, between 30 and 190. As a result, a laminar air flow model for incompressible fluid could be used. A steady-state for the air flow velocities in the street was generated using a stationary solver using a fan. The transport of the VOCs in the street was modeled by coupling the time-dependent advection and diffusion equation to the stationary velocity field vector u (Walsem 2016)

$$\frac{\partial C_{vocs}}{\partial t} = \nabla \cdot (D \nabla C_{VOCs}) - \boldsymbol{u} \cdot \nabla C_{VOCs}$$

With C_{VOCs} is the concentration of the VOCs [mol.m^{-3}] and D is the mass diffusion coefficient of the acetaldehyde as a component of VOCs in the air [m^2 s^{-1}] (Sherwood 1975, Salvadores 2016). The latter was set to 10^{-4}m^2 s^{-1} and it can be found in the literature.

Adsorption desorption of VOCs

For more in-depth description of the equations, refer to (Walsem 2016). Some equations will present to explain the adsorption/ desorption of VOCs. An important precursory step in photocatalysis is the adsorption of pollutants on the TiO_2 surface. The fractional surface coverage θ_{Acal} is determined as the ratio of the surface concentration of adsorbed molecules [mol/m^{-2}] $C_{VOCs,ads}$ and Γ_s, as defined the maximum surface coverage. In addition, θ_{Acal} can be determined by the bulk concentration C_{VOCs} and the Langmuir equilibrium constant K, with K is the ratio of the adsorption and desorption rate constants k_{ads}/k_{des} (Walsem 2016, Vorontsov 2004).

$$\theta_{Acal} = \frac{K.C_{VOC}}{1+K.C_{VOC}} = \frac{C_{ads}}{\Gamma_s}$$

Knowing only the value of Langmuir equilibrium constant K is not sufficient for an accurate modeling, for this reason it was important to use independent value for both K_{ads} and K_{des} to simulate the evolution of the pollutant concentration in the system. VOCs adsorption was modeled as a species flux N_{ads} across the coated surface of the lamellae [mol m^{-2} s^{-1}] from the street to the surface; desorption, on the other hand, was a species flux N_{des} across the same boundaries but in opposite direction.

$$-\boldsymbol{n}.(-D\nabla C_{vocs} + \boldsymbol{u}.C_{vocs}) = -N_{ads} + N_{des}$$

With n is the normal vector pointing outward on the boundaries. To ensure the conservation of mass, the same rate expressions were used for the new species Cads. The only difference is that desorption is a sink term with a negative sign and adsorption is a source term with a positive sign.

$$\frac{\partial C_{ads}}{\partial t} = N_{ads} - N_{des}$$

A uniform UV intensity distribution on the coated surfaces of the lamellae was assumed. Also, a straightforward approach was followed in which the photocatalytic reaction rate is expressed by an order one with respect to the surface concentration of adsorbed molecules (Mo 2009).

$$R_{pco} = k_{pco} C_{ads}$$

where k_{pco}[s^{-1}] is the photocatalytic reaction rate constant. The photocatalytic reaction rate R_{pco} [mol m^{-2} s^{-1}] was added to the expression for the time derivative of adsorbed acetaldehyde as an extra sink term to account for the degradation of acetaldehyde on the coated surfaces of the glass tubes during illumination.

$$\frac{\partial C_{ads}}{\partial t} = N_{ads} - N_{des} - R_{pco}$$

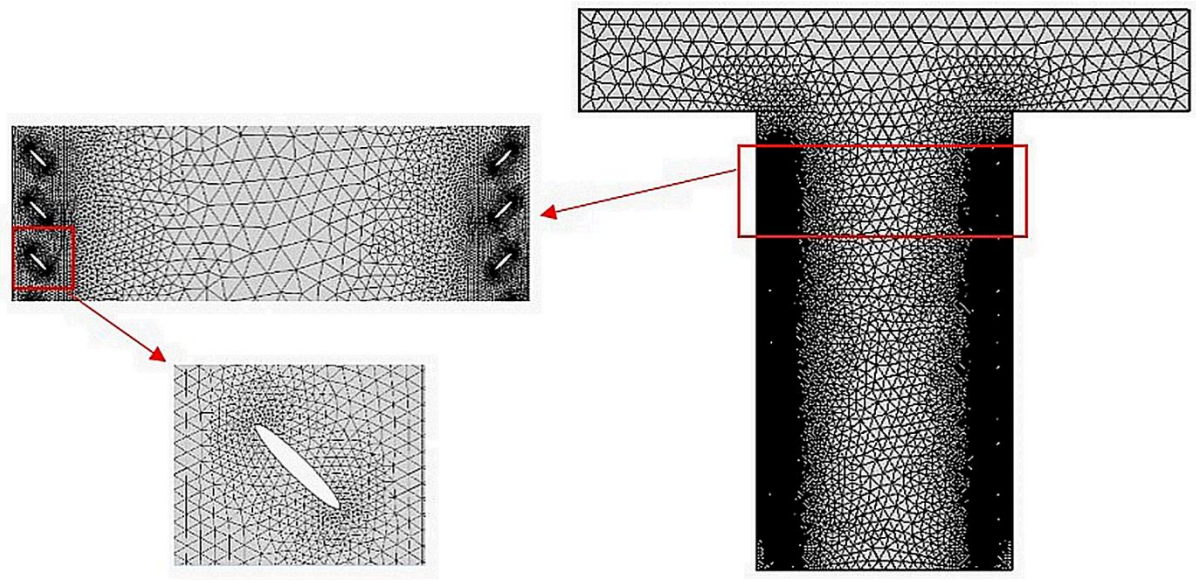

Figure 1: Representation of the mesh used in the CFD simulations

Simulation Scenarios

A large number of research studies have focused on street canyons, where the highest levels of air pollution often occur and the larger targets of impact are concentrated. Most authors have adopted different combinations of monitoring and modelling techniques for assessing air quality in urban street. There are several methods for monitoring roadside particulate and gaseous pollutants, each one of them having a number of advantages and drawbacks. Passive sampling can be used to obtain air quality data of high spatial resolution (both vertically and horizontally). On the other hand, active sampling can provide high temporal resolution. Literature and recent studies focusing on traffic related pollution show that the most important problem in urban environments such as street canyons is the lack of 'urban ventilation', causing pollutants to remain in the streets. Solutions to this are very drastic: urban design can help (but requires removing buildings, creating open space in cities). Locally, solutions using PCO might be promising. However, when using PCO one should also invest in methods to improve contact with photocatalytic surfaces. We expect that the solution to the problem is a trade-off between energy use (fans etc.) and air quality. Other systems like natural convection and solar energy (e.g., PV cells for powering fans and heating surfaces) could be a solution also. In an urban context removing the pollutants from one to another location is not a solutions, hence the need for purification.

In this context, the aim of this work is to simulate a new technology for air cleaning in street canyons. In this purpose four different streets were simulated. Those streets are known as one of the most polluted street in the city and they have different aspect ratio. For each street aspect ratio, two scenarios were tested. In the first approach, only a constant concentration background was taking in consideration. We modeled the polluted air as a constant concentration avoiding any other pollution sources as traffic, a concentration of 10^{-4} mol.m^{-3} was taking into account, it is about 2.4 ppm (for an average molecular weight of VOC 80g/mol). This is a high value, but not unusual for contaminated urban streets. This concentration could be found in the principals streets in big cities or industrial areas. Indoors, mostly values of a few 100's ppb (up to 500ppb =0.5ppm) are encountered. The VOC's concentration is not constant all the time, it depend also on the traffics in the streets, car emissions, industrial activities etc.

In the second approach, car emission was introduced in the simulation as a source continuously emitting pollutants with a concentration of 10^{-6}mol.m^{-3}.s^{-1}. By doing so, it was important to simulate under the same conditions (boundary condition and car emission) without photocatalysis reaction, in order to

compare the efficiency of the model in the two cases. The simulation without air cleaning present the evolution of the concentration of the VOC's in the normal case. In both cases, open boundaries also had the same concentrations as the initial concentration. Open boundaries represent the area outside the street.

APPLICATION OF AI AS A FORECASTING TOOL

Artificial neural networks (ANNs), are networks of simple processing elements (called 'neurons') operating on their local data and communicating with other elements. ANNs learns from training data to discover patterns and relationships between the input and the output. There are many types of ANNs but the principe is similar, each ANN consists of an input layer, one or more hidden layers of neurons and a final layer of output neurons. The input layer passes the information to the next layer. Each neuron in a particular layer is connected with all neurons in the next layer. The connection between the ith and jth neuron is characterized by the weight coefficient w_{ij} and the i_{th} neuron by the threshold coefficient ϑi (Figure 3).The weight coefficient is the degree of importance of the connection in the neural network. In the hidden layer, all the processing and computation are done. ANNs are formed from several neurons, depending on the model. Each neuron is connected with a coefficient (weight). They are known also as processing elements as they process information (Li 2017, Schmidhuber 2015). Each neuron has also a transfer function (1,2) (Srivastava 2014) and one output. The inputs of each neuron are multiplied by the connection weights, then combined and passed through a transfer function (3) (Srivastava 2014) to make the output of the neuron (Figure 3). There are many transfer functions in the literature. The output value (activity) of the ith neuron xi is determined by the equations below: (Wilamowski 2010, Fu2015)

$$x_i = s(\xi_i) \ (1)$$

$$\xi_i = \vartheta_i + \sum \omega_{ij} x_j \ (2)$$

$$\psi(x) = \frac{1}{1+e^{-x}} \ (3)$$

where ξi is the potential of the ith neuron and $\psi(x)$ is the sigmoid function

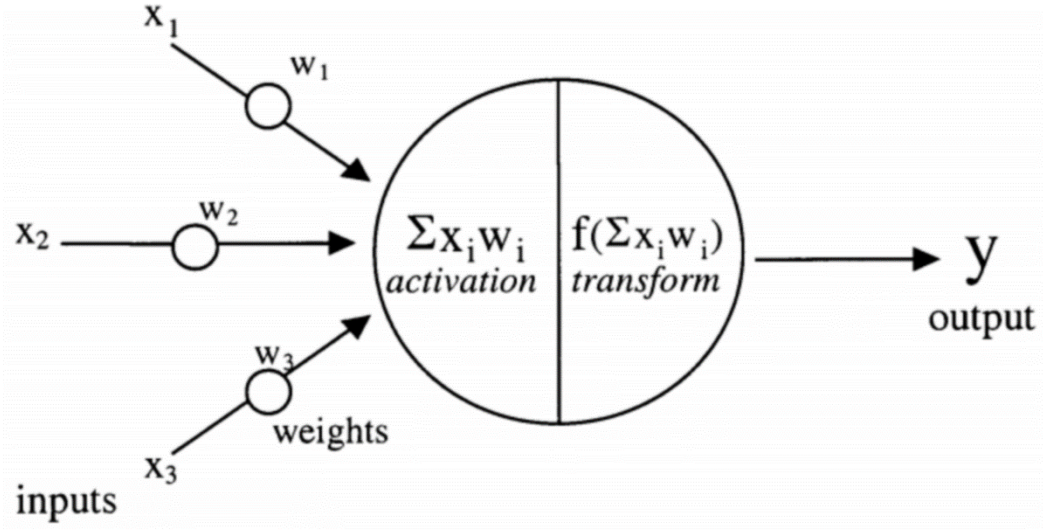

Figure 3:Typical structure of a feed-forward neural network.

Neural network model

The model is based on a feed-forward neural network, with back propagation, it's a simple model from the literature. That kind of ANNs should at least have three layers, an input layer, a hidden layer, and an output layer. Appropriate selection of the number of hidden layers, and neurons in each of them needs experimentation. In this network, there no cycles nor loops, and the information moves in only one direction. Given a dataset with N distinct samples $\{x_i,t_i\}_{i=1}^{N}$ where the inputs $x_i \in Rn$ and the the outputs $t_i \in Rm$, the NN with K hidden nodes and activation function $\psi(.)$ for approximating the N samples can be expressed by (Wan 2015)

$$f_k(x_j) = \sum_{i=1}^{k} \beta_i \psi(a_i . x_j + b_i), \;\; j = 1,2 \ldots . , N \; (4)$$

Where a_i denotes the weight vector between the ith hidden neuron and the input neurons, β_i is the weight vector between the ith hidden neuron and the output neurons, bi represents the threshold of the ith hidden node, and $\psi(a_i \cdot x_j + b_i)$ is the output of the ith hidden node with respect to the input x_j. Theoretically, the parameters of NN can be optimized through different algorithms, among which the back propagation (BP) algorithm is the most common gradient-based algorithm with the objective function defined by: (Wan 15)

$$C = \sum_{j=1}^{N} \left(\sum_{i=1}^{K} \beta_i \psi(a_i . x_j + b_i) - t_j \right)^2 \; (5)$$

Once the error is less or equal to the threshold value, the test set of data is used by the trained neural network with the new weights to test the performance of the neural network. This step is important to see how well the network is good and to test the ability to predict the output with the minimum error possible using the adjusted weight of the network. After that, the network is trained (with the training set) and tested (with the test set), then it becomes ready to make predictions. It's possible to feed it with some new input to produce the predicted output.

In order to minimize the error, the weight of each node needs to be updated. Back propagation algorithm looks for the minimum value of the error function in weight space using a technique called the delta rule or gradient descent through calculating the derivative of the error function. For more in-depth description of the back propagation rule refer to (Lippmann 1987, Srivastava 2014 , Basheer 2000). The ANN was trained using the Levenverg-Marquardt algorithm, a standard training algorithm from the literature. It is fast and has stable convergence, as it combines the gradient descent and the Gauss-Newton algorithms. The Levenberg–Marquardt(LM) algorithm is remarkably efficient and strongly recommended for neural network training (Wilamowski 2010, Fu 2015). Eight training algorithms were used to compare the results based on the training time, number of iterations and Mean Squared Error (MSE). One single hidden layer was used in this network with a number of neurons (5, 10, 20). The hyperbolic-tangent-sigmoid function was used as a transfer function. Levenberg-Marquardt algorithms gives the less error comparing to other algorithms, so it was used to train the model. The Mean Squared Error is the minimization criteria.

$$MSE = \frac{1}{N} \sum_{i=1}^{N} (\widehat{X_i} - X_i)^2$$

To avoid the problem of overfitting, cross-validation can be used. The main idea is to use the initial training data to generate mini train-test splits where those splits will be used to tune the model. Cross-validation is a powerful preventative measure against overfitting because it allows tuning hyper parameters with only the original training test. Early stopping is also a solution for the overfitting problem and it is based on dividing data into two sets, training and validation, and computing the validation error periodically during training. Training is stopped when the validation error rate starts to go up (Khryashchev).

Three neurons in the input layer were used, two for the coordinate of each point of the street and the third for the time step. The output consists of one neuron presenting the concentration of the VOCs, and five neurons was used in the hidden layers for calculations (4,5)(Figure 4).

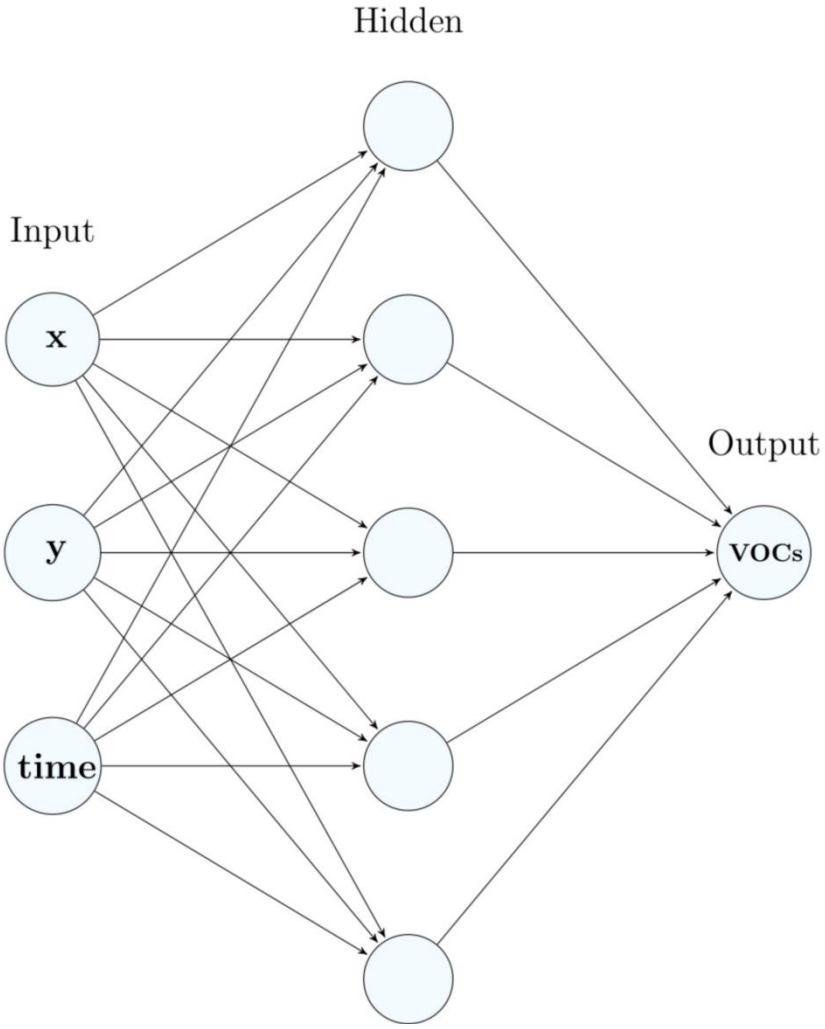

Figur4: Artificial Neural Network architecture used for five neurons in a single hidden layer.

Dataset Details

The training data of the model was collected from the simulation results in Comsol Multiphysics. Only one simulation was taken into account, because of the amount of data. The simulation of a street with an aspect ratio of 1.8 with a constant concentration was used to feed the model. Comsol software was used to create a mesh to export data, with a distance of 10 cm between two points. Different Comsol models were used in this work, computational fluid dynamics(CFD) model was used to simulate the air flow in the system, then, transport of diluted species (tds) was used for the chemical reactions and the photocatalysis reactions. Afterwards the data was exported to Matlab using LiveLink for Matlab. LiveLink for Matlab is a model provided by Comsol to make a link between the two software, in order to export the simulation models, data and also use Matlab functions in Comsol. The choice of Matlab can be explained by the tools provided by Comsol to export the data, also Matlab provides tools to create ANN models with different training algorithms; The final dataset consists of the coordinate x and y of each point and the concentration of VOCs recorded for six hours, with a time step of 1 minute. The dataset was randomly divided into three sets. Training set consists of 70% of the data used to train the model, 15%

samples as validation data to measure the generalization of the network by feeding it with data it has not seen before. The rest of the data is called test data; it is used for an independent measure of the performance of the neural network in terms of MSE (Mean Squared Error). It is the square difference between the predicted value and the target and it is always a positive value.

Learning and Forecasting Procedures

The Neural Network Fitting Tool GUI nn tool available in MATLAB (R2017a) is used to carry out the analysis on the purification data from the previous simulations. The only simulation data that was used is the case of a street with an aspect ratio of 1.8 with a constant VOCs concentration background. An artificial Feed-Forward neural network was used and it was trained with Levenberg-Marquardt algorithm for back propagation. The network contained three neurons in the input layers, one hidden layer with 10 neurons and the output layer contained one neuron, and the concentration of VOCs presented the target of the network

DISCUSSION AND RESULTS

Simulation results

Air flow

A stationary solver was used to simulate the air flow generated by forced convection. A typical steady-state is plotted (Figure 4). Three different flow rates were used in this work 0.1 m^3/s, 0.5 m^3/s and 1m^3/s to test the impact of the air flow in the process. The highest velocity was recorded near to the fans in two sides; it can be explained by the fact that in these places the air flow did not get in touch with any obstacle yet to reduce the velocity. The maximum velocity in the sides of the fans was (resp. 0.4, 2.3, 3.92 m/s). The lowest velocity was located inside the street; less than 0.4 m/s was recorded and the velocity in the system varies between 0.5m/s and 1.5 m/s. The velocity profile depends on the location, the distance from the fan, the fan used, the pressure and also the flow rate.

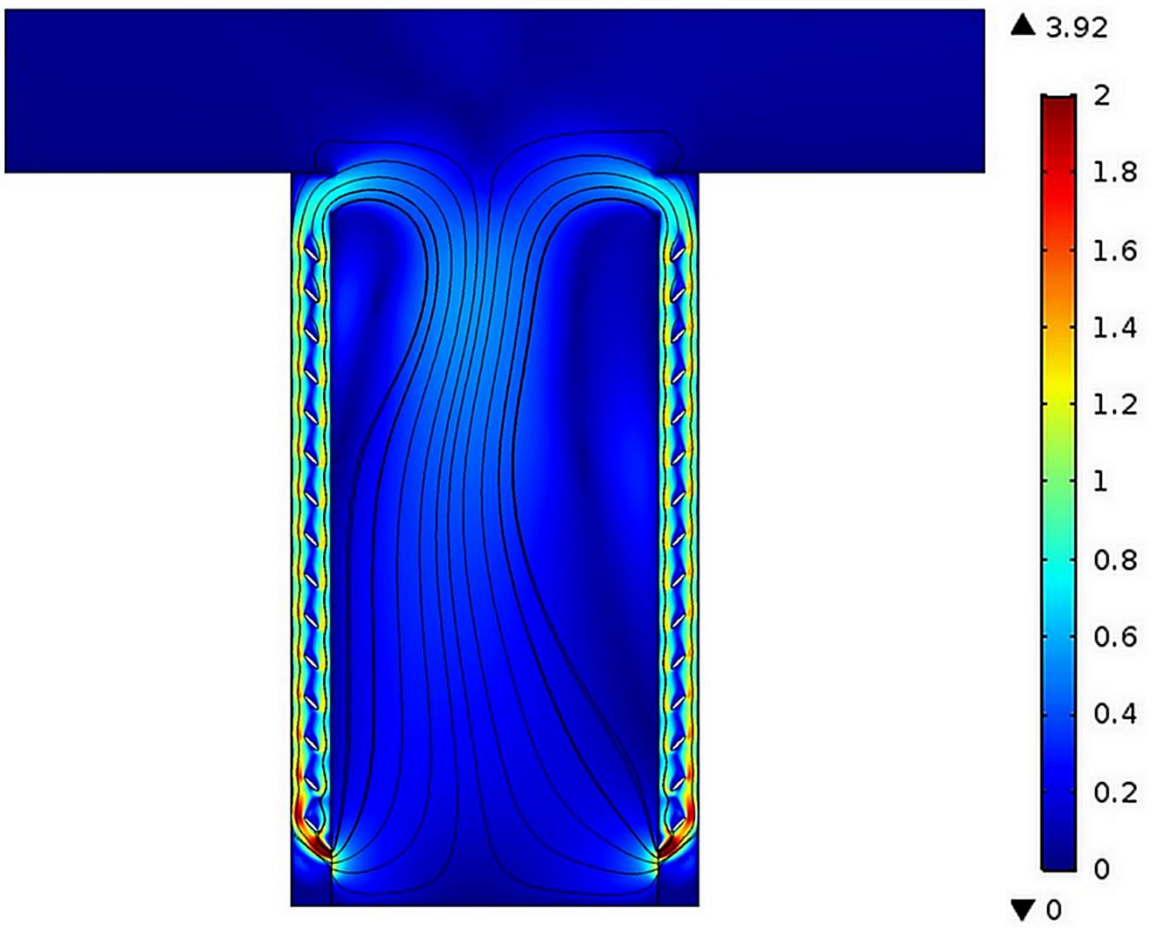

Figure 5: Modeled velocity profile in the street using a fan for the air flow

VOC's concentration modelling

The evolution of the VOCs concentration is modeled by coupling the time dependent advection and diffusion equation to the stationary velocity. Four different street aspect ratios with both constant concentration background and car emission were tested but only one case will be presented. A street with an aspect ratio of 1.8 (the dimensions of the street are Height=18m and Width=10m). We mention that a full-scale simulation was made.

Figure 6 presents the evolution of the concentration of VOCs in the street for different time steps. At the beginning of the simulation, the concentration was the same 10^{-4} mol.m-3 in each point of the street and the system. After running the fans in the two sides, the fans create an air flow in the street, but especially between the lamellae. Once the air gets in contact with the coated surfaces, with the presence of the UV light, the molecules are broken down into water and CO_2. This process reduces the VOCs concentration and makes the air more purified. The purified air follows the same velocity streamline, and it turns back to the street, minimizing the amount the VOCs there. By the time the purified air gradually replaces the polluted air (4 hours), after that a steady state is achieved. The velocity of the air flow affects the results, for this reason it was important to test different fans with different flow rate. The more the air gets in contact with the coated surfaces, the more it reduces the VOCs by breaking them down.

Figure 7 presents the average concentration in the street during the simulation time using the three fans flow rate. The concentration average decreases differently with each case. A low percentage of purification can be achieved with a low flow rate of 38%, while a high flow rate can provide more

purification 65% which can be explained by the amount of the VOCs molecules adsorbed by the coated lamellae and the movement of the air in the street and between the lamellae that moves the pollutants molecules. In all the cases, the concentration average gets lower and lower until a stationary state is established. A balance between open boundaries, fan and purification were found after several hours of simulation.

Figure 8 presents a summary of all the simulations made with a constant concentration background. It presents the concentration averages for each aspect ratio testing different methods. Comsol Multiphysics provides a tool to calculate the average of each species in every time step. For every aspect ratio, the flow rate affects the purification percentage. It increases the amount of adsorbed molecules by the coated surfaces, thus break down more VOCs molecules. The purified air returns back to the street creating a loop that reduces the concentration of the polluted in the street.

Figure 9 shows the average concentration of the VOCs in all the simulations that introduce the car emissions as a source continuously emitting pollutants. The velocity of the air flow affect also, in this case, the purification percentage for the same reason explained before. In all the aspect ratio, high flow rates result high purification percentage, due to the high amount of air get in contact with the coated lamellae. In all case, over 60% of purification could be achieved if we used a powerful fan.

The goal of this work is to find the method that gives the best purification percentage. But this method needs to be environmentally friendly by reducing the energy cost of the solution. So it was required to take into account the energy consumption of the method. A comparison was made based on the efficiency of the method and the energy cost. In both cases, commercial fans with the same characteristics were used in the comparison. A high purification percentage 65% cost around 780W. While reducing the energy cost of the method to 250W reduces the purification percentage to only 38 %.

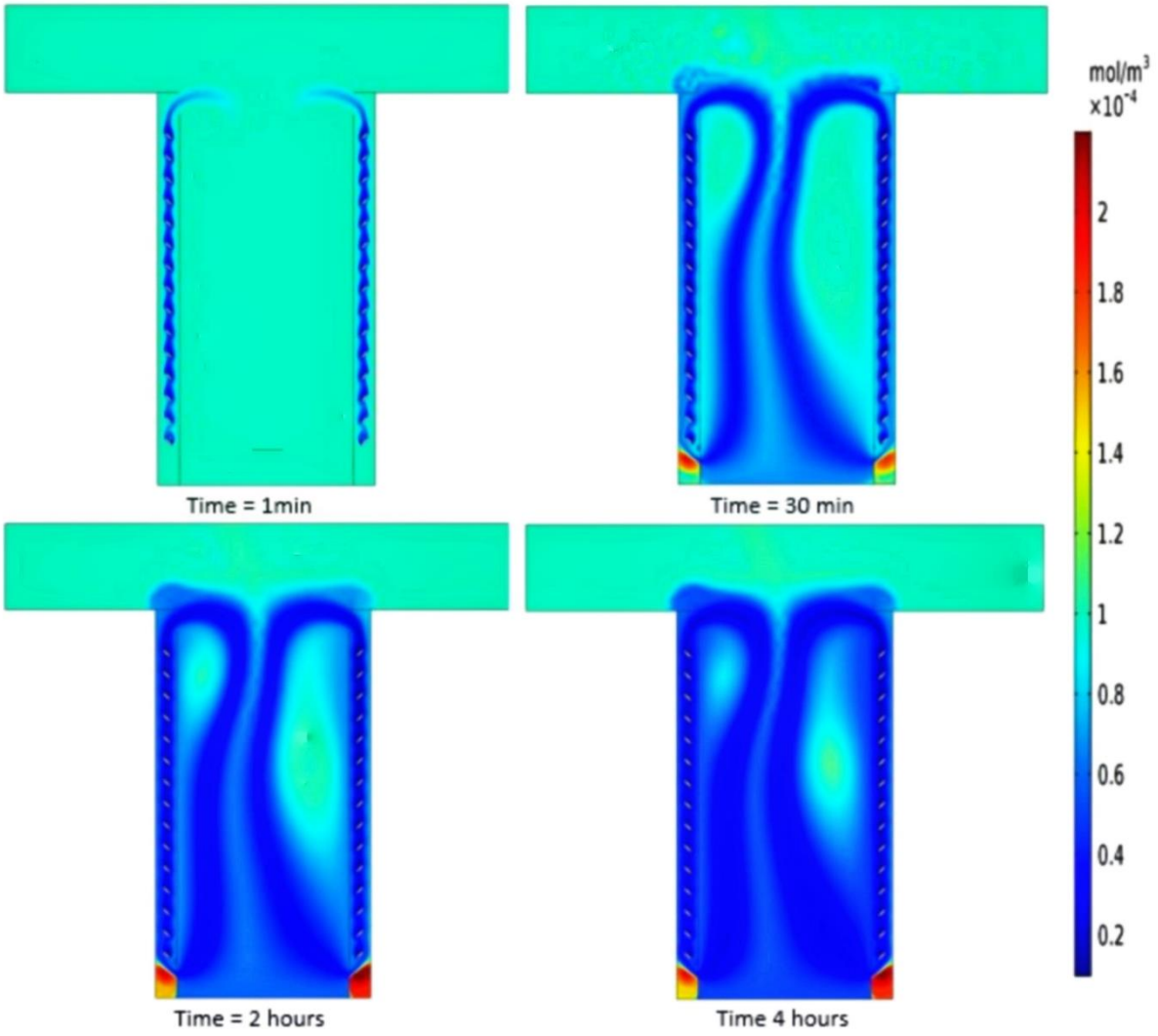

Figure 6: Evolution of the concentration during the simulation time

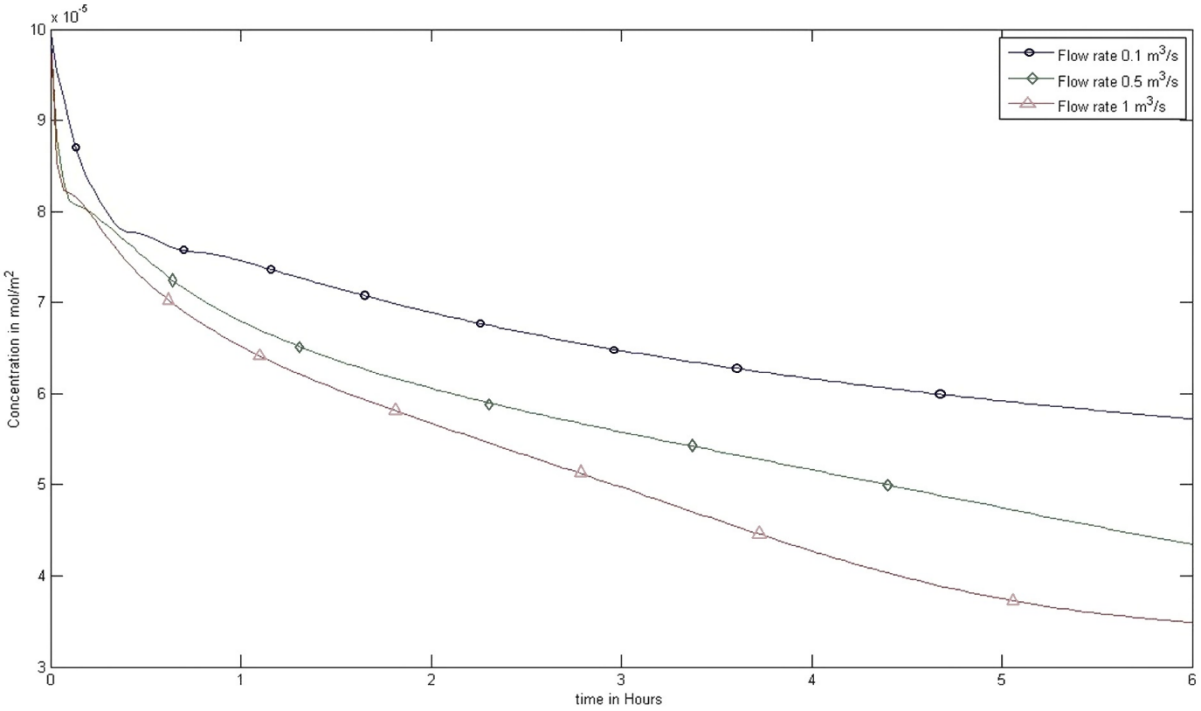

Figure 7: Average concentration of VOCs with different flow rate for a street with an aspect ratio of 1.8

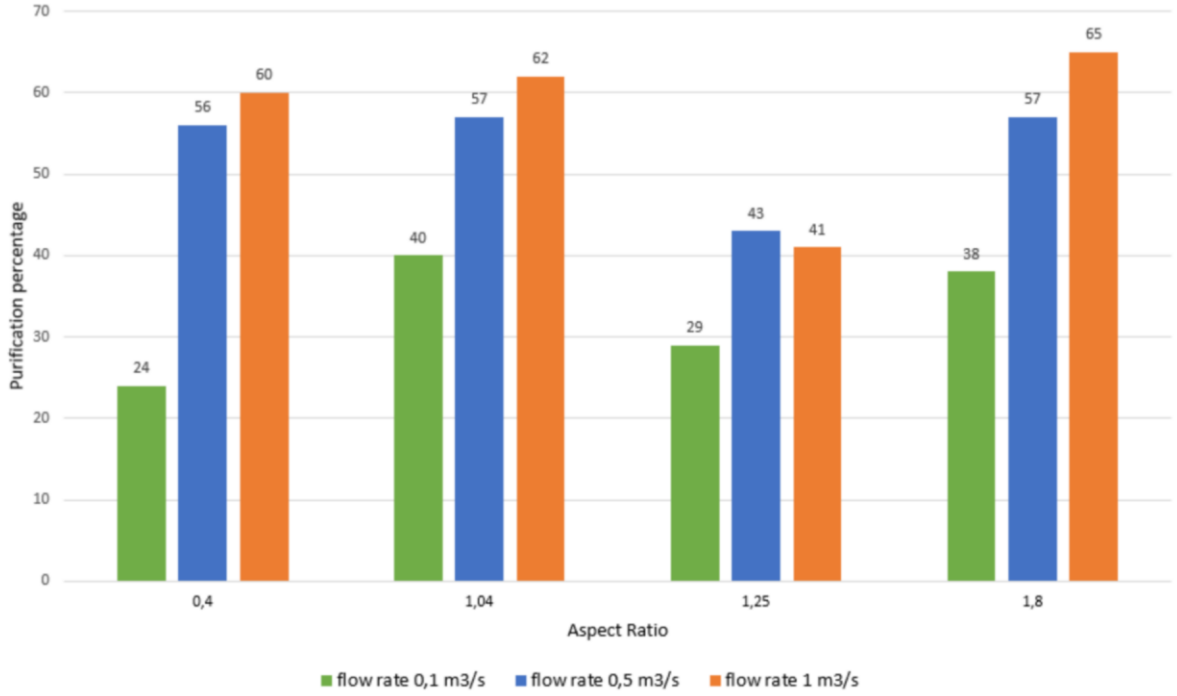

Figure 8: Purification percentage for different street aspect ratio testing different flow rate, with a constant concentration.

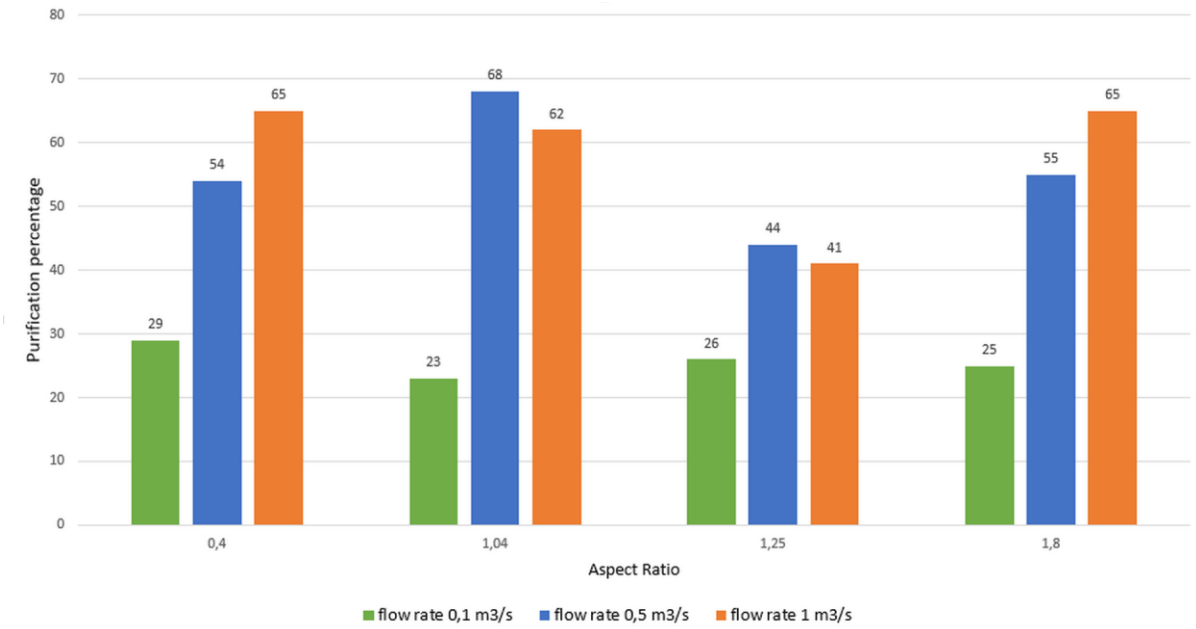

Figure 9: Purification percentage for different street aspect ratio test different flow rate, with a continuous emitting source.

Artificial Intelligence methods results

In the first approach, polynomial regression was used to predict the best purification method. Regression analysis is usually carried out under the hypothesis that one of the variables is normally distributed with constant variance, its mean being a function of the other variables. Polynomial of Degree n would look like:

$$Y = b_0 + b_1 x_1 + b_2 x_2^2 \ldots + b_n x_n^n$$

where Y caret is the predicted outcome value for the polynomial model with regression coefficients b1 to bn for each degree and Y intercept b0. The model is simply a general linear regression model with n predictors raised to the power of i where i=1 to n.

The steady-state concentration is modeled as an nth degree polynomial. 15 polynomials were tested. The optimal polynomial was chosen based on the error. The degree 13 gives the best results. The choice was validated by comparing the given results from polynomial regression with other results from Comsol. By running a simulation for a new aspect ratio, the model gives error between 0.1% and 0.3%. The results were used to decide the best purification method, by comparing the efficiency of the solution and the consumed energy. (Figure 10) presents the graphical interface developed with Matlab for this solution. The graphical interface shows the predicted purification percentage of the new street aspect ratio and the energy cost. The blue lines present the simulation data and the red dotes are the predicted percentage. The interface calculi also the energy cost of the solution based on similar fan in the market with the same characteristics.

In the second approach, different training algorithms could be used to train the neuron network. The ANN was used to investigate the possibility of reduction of the calculation time, which is long if we want to simulate the solution for a city with hundred streets. (Figure 11) presents a comparison between nine training algorithms. The Levenberg-Marquardt algorithm gives less Mean Square Error(MSE) comparing to others. But it takes around 38 minutes to train the model, using a computer with 4 cores and 12 GB in RAM. The Levenberg-Marquardt algorithm was used to train the model and then, used to predict the concentration for a new aspect ratio. The choice of this algorithm was based on the MSE. LM algorithm

combines the advantages of gradient-descent and Gauss-Newton methods. The use of artificial neural network to predict the evolution of the concentration is beneficial to reduce the calculation time. It allows reducing extremely the simulation time. For example to simulate 2 hours of outdoor air purification will take at least 50 minutes using Comsol Multiphysics. But using a trained network with Levenberg-Marquardt algorithm the prediction will take only 20 seconds with a mean square error of $3.1.10^{-8}$. Time reduction present 144 times acceleration ratio. Therefore, the use of ANN to simulate emission concentration would be an original and good option to design an air purification strategy for different streets aspect ratio and to propose consequently an optimal solution for a cleaner city.

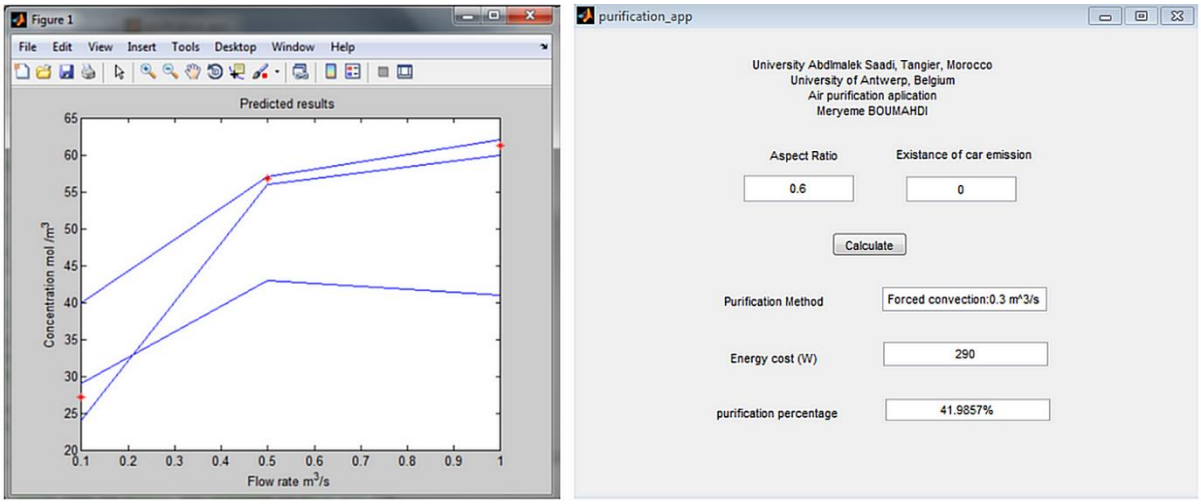

Figure 10: Prediction of the steady-state concentration after purification with the best purification method and the energy cost.

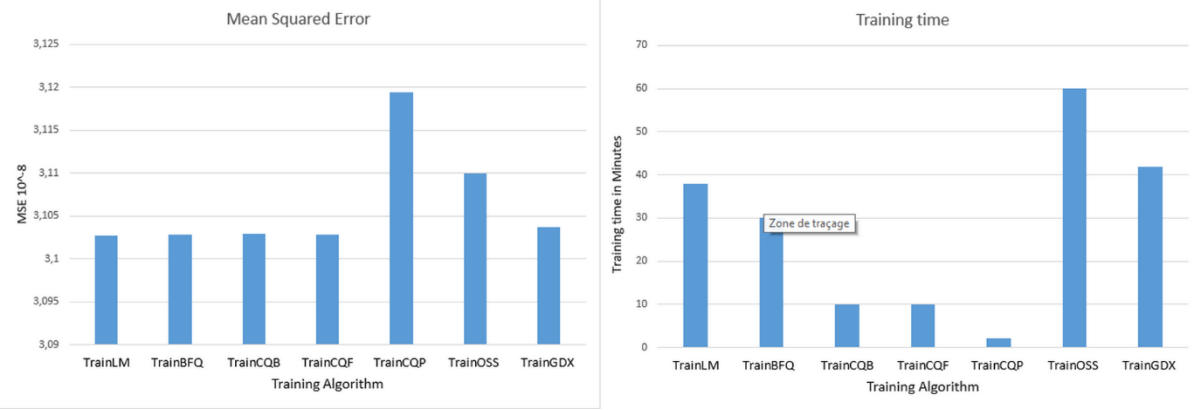

Figure 11: Training algorithms and related performance

CONCLUSION

The aim of this work was to present a new and innovative outdoor air purification solution. The solution was based on TiO2 coated lamellae. Photocatalysis was used to break down the molecules of VOCs, reduce concentration and clean the air. Different strategies and cases have been tested and car traffic as a continuous source of emission has also been taken into account. In this system, several physics and chemistry equations have been combined. The results of the simulations showed a good percentage of purification. The percentage depends on the air velocity where a high percentage of air flow is required. High flow rate fans are required in order to achieve this airflow. The air cleaning percentage can achieve 65% of clearing with a fan with a flow rate of 1 m^3s^{-1}.

At the end of the simulation tasks, polynomial regression and artificial neuron network were used to predict the purification percentage for new streets and to choose the best purification strategy based on

the efficiency and the energy cost. Polynomial regression has been used to determine an optimized new aspect ratio purification scenario.
The artificial neural network was used to predict the development of new street concentration. The simulation output has been used to train the forecasting model. The model is based on a neural feed-forward network with back spread. In this work, nine different training algorithms were tested. The model was trained with the ML algorithm, based on the MSE and the training.
The network could be used to predict the concentration for a new aspect ratio as the mean square error obtained is $3.1.10^{-8}$. The ANN model also reduces the calculation time, the time reduction has a speed ratio of 144 times. This study was the first attempt to model a new outdoor air pollution solution.
For future research, real weather conditions and pollution concentrations, obtained from soil sensors or satellite data, could be taken into account in the purification process and other artificial intelligence methods as a deep leaning to obtain better results.

ACKNOWLEDGMENT

The authors of this work are thankful to VLIR-UOS for the financial support provided within the project ZEIN 2016Z193.

REFERENCES

Kurt, O. K., Zhang, J., & Pinkerton, K. E. (2016). Pulmonary health effects of air pollution. *Current opinion in pulmonary medicine*, *22*(2), 138.
Li, Y., Li, Y., Zhou, Y., Shi, Y., & Zhu, X. (2012). Investigation of a coupling model of coordination between urbanization and the environment. Journal of environmental management, 98, 127-133.
Li, X., Qiao, Y., & Shi, L. (2017). The aggregate effect of air pollution regulation on CO2 mitigation in China's manufacturing industry: an econometric analysis. *Journal of Cleaner Production*, *142*, 976-984.
B. Brunekreef, S. T. Holgate, Air pollution and health, The lancet 360 (9341) (2002) 1233–1242.
D'Amato, G., Pawankar, R., Vitale, C., Lanza, M., Molino, A., Stanziola, A., ... & D'Amato, M. (2016). Climate change and air pollution: effects on respiratory allergy. *Allergy, asthma & immunology research*, *8*(5), 391-395.
Kelly, F. J., & Fussell, J. C. (2015). Air pollution and public health: emerging hazards and improved understanding of risk. Environmental geochemistry and health, 37(4), 631-649.
Paz, Y. (2010). Application of TiO2 photocatalysis for air treatment: Patents' overview. Applied Catalysis B: Environmental, 99(3-4), 448-460.
Mamaghani, A. H., Haghighat, F., & Lee, C. S. (2017). Photocatalytic oxidation technology for indoor environment air purification: the state-of-the-art. *Applied Catalysis B: Environmental*, *203*, 247-269.
P. C. Ribeiro, A. C. F. d. M. Costa, R. H. G. A. Kiminami, J. M. Sasaki, H. L. Lira, et al., Synthesis of tio2 by the pechini method and photocatalytic degradation of methyl red, Materials Research 16 (2) (2013) 468– 472.
Bianchi, C. L., Pirola, C., Galli, F., Cerrato, G., Morandi, S., & Capucci, V. (2015). Pigmentary TiO2: A challenge for its use as photocatalyst in NOx air purification. *Chemical Engineering Journal*, *261*, 76-82.
Zhao, J., & Yang, X. (2003). Photocatalytic oxidation for indoor air purification: a literature review. *Building and Environment*, *38*(5), 645-654.
Dayhoff, J. E., & DeLeo, J. M. (2001). Artificial neural networks. Cancer, 91(S8), 1615-1635.
Wang, S. C. (2003). Artificial neural network. In Interdisciplinary computing in java programming (pp. 81-100). Springer, Boston, MA.
White, H. (1989). Learning in artificial neural networks: A statistical perspective. Neural computation, 1(4), 425-464.
Adebiyi, A. A., Adewumi, A. O., & Ayo, C. K. (2014). Comparison of ARIMA and artificial neural networks models for stock price prediction. *Journal of Applied Mathematics*, *2014*.

Lapedes, A., & Farber, R. (1987). Nonlinear signal processing using neural networks: Prediction and system modelling (No. LA-UR-87-2662; CONF-8706130-4).
Hanna, S. R. et al. Detailed Simulations of Atmospheric Flow and Dispersion in Downtown Manhattan: An Application of Five Computational Fluid Dynamics Models. Bull. Am. Meteorol. Soc. (2006).
Buccolieri, R. et al. Analysis of local scale tree-atmosphere interaction on pollutant concentration in idealized street canyons and application to a real urban junction. Atmos. Environ. (2011).
Toparlar, Y., Blocken, B., Maiheu, B. & van Heijst, G. J. F. A review on the CFD analysis of urban microclimate. Renew. Sustain. Energy Rev. (2017).
Murakami, S. Current status and future trends in computational wind engineering. J. Wind Eng. Ind. Aerodyn. (1997).
Zhong, J., Cai, X. M. & Bloss, W. J. Coupling dynamics and chemistry in the air pollution modelling of street canyons: A review. Environ. Pollut. (2016).
Blocken, B., Stathopoulos, T. & van Beeck, J. P. A. J. Pedestrian-level wind conditions around buildings: Review of wind-tunnel and CFD techniques and their accuracy for wind comfort assessment. Build. Environ. (2016).
García-Sánchez, C., van Beeck, J. & Gorlé, C. Predictive large eddy simulations for urban flows: Challenges and opportunities. Build. Environ. (2018).
J. van Walsem, S. W. Verbruggen, B. Modde, S. Lenaerts, S. Denys, Cfd investigation of a multi-tube photocatalytic reactor in non-steady-state conditions, Chemical Engineering Journal 304 (2016) 808–816.
T. K. Sherwood, R. L. Pigford, C. R. Wilke, Mass transfer, McGraw-Hill, 1975.
Salvadores, F., Minen, R. I., Carballada, J., Alfano, O. M., & Ballari, M. M. (2016). Kinetic study of acetaldehyde degradation applying visible light photocatalysis. *Chemical Engineering & Technology*, *39*(1), 166-174.
A. V. Vorontsov, V. P. Dubovitskaya, Selectivity of photocatalytic oxidation of gaseous ethanol over pure and modified tio 2, Journal of Catalysis 221 (1) (2004) 102–109.
Agatonovic-Kustrin, S., & Beresford, R. (2000). Basic concepts of artificial neural network (ANN) modeling and its application in pharmaceutical research. Journal of pharmaceutical and biomedical analysis, 22(5), 717-727.
Li, H., Zhang, Z., & Liu, Z. (2017). Application of artificial neural networks for catalysis: a review. *Catalysts*, *7*(10), 306.
Schmidhuber, J. (2015). Deep learning in neural networks: An overview. *Neural networks*, *61*, 85-117.
Lippmann, R. (1987). An introduction to computing with neural nets. IEEE Assp magazine, 4(2), 4-22
Srivastava, N., Hinton, G., Krizhevsky, A., Sutskever, I., & Salakhutdinov, R. (2014). Dropout: a simple way to prevent neural networks from overfitting. *The Journal of Machine Learning Research*, *15*(1), 1929-1958.
Basheer, I. A., & Hajmeer, M. (2000). Artificial neural networks: fundamentals, computing, design, and application. *Journal of microbiological methods*, *43*(1), 3-31.
Wilamowski, B. M., & Yu, H. (2010). Improved computation for Levenberg–Marquardt training. IEEE transactions on neural networks, 21(6), 930-937.
Fu, X., Li, S., Fairbank, M., Wunsch, D. C., & Alonso, E. (2015). Training recurrent neural networks with the Levenberg–Marquardt algorithm for optimal control of a grid-connected converter. *IEEE transactions on neural networks and learning systems*, *26*(9), 1900-1912.
Blocken, B. LES over RANS in building simulation for outdoor and indoor applications : A foregone conclusion ? Build. Simul. (2018).
Schatzmann, M., Olesen, H. & Franke, J. Cost 732 Model Evaluation Case Studies : Approach and Results. (2010).
Sottile, F., Caceres, M. A., & Spirito, M. A. (2012). A Simulation Tool for Real-Time Hybrid-Cooperative Positioning Algorithms. *International Journal of Embedded and Real-Time Communication Systems (IJERTCS)*, *3*(3), 67-87.

Ivanovsky, L., Khryashchev, V., Lebedev, A., & Kosterin, I. (2017, November). Facial expression recognition algorithm based on deep convolution neural network. In *Open Innovations Association (FRUCT), 2017 21st Conference of*(pp. 141-147). IEEE. Boonen, E., & Beeldens, A. (2014). Recent photocatalytic applications for air purification in Belgium. *Coatings*, *4*(3), 553-573.
Nath, R. K., Zain, M. F. M., & Jamil, M. (2016). An environment-friendly solution for indoor air purification by using renewable photocatalysts in concrete: A review. *Renewable and Sustainable Energy Reviews*, *62*, 1184-1194.
Chen, J., & Poon, C. S. (2009). Photocatalytic construction and building materials: from fundamentals to applications. *Building and environment*, *44*(9), 1899-1906.
Srivastava, A. (2015). Photocatalytic application of titanium dioxide in architectural concrete: A review. *International Journal of Scientific Research & Chemical Engineering*, *1*(1).
Khryashchev, V., Pavlov, V., Priorov, A., & Kazina, E. (2018, May). Convolutional Neural Network for Satellite Imagery. In *Proceedings of the 22th Conference of Open Innovations Association FRUCT'22* (pp. 344-347).Wan, C., Zhao, J., Song, Y., Xu, Z., Lin, J., & Hu, Z. (2015). Photovoltaic and solar power forecasting for smart grid energy management. *CSEE Journal of Power and Energy Systems*, *1*(4), 38-46.
Mo, J., Zhang, Y., Xu, Q., Lamson, J. J., & Zhao, R. (2009). Photocatalytic purification of volatile organic compounds in indoor air: a literature review. *Atmospheric environment*, *43*(14), 2229-2246.